1   **Title:**

2   **Contribution of *rsaC*, a small non-coding RNA, towards the pathogenicity of *Staphylococcus***

3   ***aureus* in a mouse systemic infection model**

4

5   Suresh Panthee[1,#], Hiroshi Hamamoto[2,3,#], Atmika Paudel[4], Suguru Ohgi[5,6], Kazuhisa Sekimizu[1,7,*]

6   [1] Drug Discoveries by Silkworm Models, Faculty of Pharma-Science, Teikyo University, Tokyo,

7   Japan.

8   [2] Teikyo University Institute of Medical Mycology, Tokyo, Japan.

9   [3] Division of Sport and Health Science, Graduate School of Medical Care and Technology, Teikyo

10 University, Tokyo, Japan.

11 [4] International Institute for Zoonosis Control, Hokkaido University, Sapporo, Japan.

12 [5] Laboratory of Microbiology, Graduate School of Pharmaceutical Sciences, The University of

13 Tokyo, 7-3-1 Hongo, Bunkyo-ku, Tokyo 111-0033, Japan

14 [7] Genome Pharmaceuticals Institute, Ltd, Tokyo, Japan.

15 [6] Current address

16 Kyowa Kirin Co., Ltd., 1-9-2 Otemachi, Chiyoda-ku, Tokyo 100-0004, Japan

17 * correspondence: sekimizu@main.teikyo-u.ac.jp

18 [#] These authors contributed equally

19

20 **Running title:**

21 sRNA *rsaC* is required for full virulence of *S. aureus*

22

23 **Keywords:**

24 *Staphylococcus aureus*, Transcriptome analysis, virulence, sRNA, *in vivo*, pathogenicity

25

26

1

Abstract

Understanding how a pathogen responds to the host stimuli and succeeds in causing disease is crucial for developing a novel treatment approach against the pathogen. Transcriptomic analysis facilitated by RNA-Seq technologies is used to examine bacterial responses at the global level. However, the ability to understand pathogen behavior inside the host tissues is hindered by much lower pathogen biomass than host tissue. Recently, we succeeded in establishing a method to enrich *Staphylococcus aureus* cells from infected organs. In this research, we analyzed the small non-coding RNA (sRNA) transcriptome of *S. aureus* inside the host and found that *rsaC* was among the highly expressed sRNAs. Furthermore, by gene disruption and complementation, we demonstrated that *rsaC* was required for full pathogenicity of *S. aureus* in a murine model. Besides, we found that Δ*rsaC* showed a difference in gene expression depending on the oxygen and host stress. The findings of this study suggest *rsaC* acts as a novel virulence factor in *S. aureus* and might facilitate the adaptation of *staphylococci* within the host.

Importance

Drug-resistant *Staphylococcus aureus* is among the pathogen for which new treatment options are urgently needed. However, limited understanding of *S. aureus* pathogenesis in the host has hindered unearthing potential strategies to treat the infections. Here, based on the *in vivo* transcriptomic analysis, we present the identification of a small non-coding RNA (sRNA) *rsaC* as a novel virulence factor of *S. aureus*. Furthermore, we performed transcriptomic analysis of the *rsaC* disrupted mutant and identified different pathways, possibly controlled by *rsaC*, during aerobic, anaerobic, and *in vivo* conditions. These findings contribute to reveal the role of sRNA *rsaC* and broadens our understanding of the adaptation of *S. aureus* to host environments.

Text

51

52   The growth and behavior of a pathogenic microorganism differ between the host

53   environment and in the *in vitro* culture. Understanding how a pathogen responds to the host stimuli

54   and succeeds in causing disease is crucial for developing novel drugs against the pathogen.

55   Comprehensive transcriptomic analysis facilitated by RNA-Seq technologies using next-generation

56   sequencers has been widely used to understand pathogen response at the global level (1, 2). Several

57   studies have used *in vitro* host-like or *in vivo* host environments to understand the infection process

58   and alterations in the pathogen and the host (3, 4). Such studies aimed to elucidate the functional

59   role of protein-coding genes, while the small non-coding RNAs (sRNAs) remain largely unattended.

60   Studies that performed the comparative analysis of pathogen response in the host to the in vitro

61   growth allowed us to evaluate how a pathogen behaves during infection situations and how the host

62   responds to pathogen invasion (4-7). The current understanding of bacterial pathogenesis allowed

63   us to identify key virulence determinants that could potentially be exploited as a drug target for

64   antivirulence drugs. Whereas it can be expected that pathogens lacking these virulence factors are

65   easy to be killed or cleared from the host, their behavior in the host has not been analyzed at the

66   global level. Furthermore, a detailed evaluation of pathogenesis requires an understanding of

67   pathogen behavior during actual infection conditions.

68

69   sRNAs have been identified in living organisms, including the bacterial kingdom. Although

70   they do not encode functional proteins, they can accomplish a wide range of biological functions,

71   including regulation of gene expression at the levels of transcription, RNA processing, mRNA

72   stability, and translation (8). In bacteria, sRNAs have the potential to regulate the gene expression

73   pattern of the bacteria by interacting with protein or mRNAs by cis- or trans-acting mechanisms (8),

74   thus affecting multiple cellular processes such as pathogenesis and bacterial physiology in response

75   to environmental cues, facilitating survival under unfavorable environments. In *Staphylococcus*

76   *aureus*, a pathogen of global concern, several sRNAs have been identified (9-11), while the

77   functional characterization of this class of RNAs has long been forsaken. One of the functionally

78   characterized and extensively studied Staphylococcal sRNA, RNAIII, regulates the expression of

79   several virulence factors both positively and negatively (12-14). *rsaC*, a part of polycistronic operon

80   *mntABC*, is another staphylococcal sRNA known to be expressed in infected host (15) and modulate

81   oxidative stress during manganese starvation (16). Whereas these studies provided a hint towards its

82   role in *S. aureus* virulence, a cell-based study showed that the Δ*rsaC* strain was more persistent in

83   macrophages and resistant to opsonophagocytosis than the wild-type strain (16) indicating its

84   obscure role in pathogenesis.

85

86   We recently successfully enriched pathogen RNA from an infected animal and performed an
87 *in vivo* RNA-Seq analysis of *Streptococcus pyogenes* (5) and *S. aureus* (6) using a two-step cell
88 crush method. In this manuscript, we performed the comprehensive analysis of *S. aureus* sRNAs
89 expressed within the host. Using RNA-Seq analysis of the *rsaC* disrupted mutant, we showed a
90 clear difference between the gene expression patterns during *in vivo* and *in vitro* (aerobic and
91 anaerobic) growth conditions. Furthermore, we found that the transcription of fermentation and
92 oxidoreductase-related genes, virulence and toxin-related genes, and host evasion-related genes
93 were affected during aerobic, anaerobic, and *in vivo* growth, respectively. Our results highlight the
94 importance of *in vivo* transcriptomic analyses of two strains with the same genetic background to
95 allow a direct comparison, revealing changes in different environments.

96

97 **Materials and Methods**

98 **Ethics statement**

99   All mouse experiments were performed at the University of Tokyo and Teikyo University,
100 following the animal care and use regulations approved by the Animal Use Committee (approval
101 numbers: P27-4 and 16-014 at respective institutes).

102

103 **Bacterial strains and primers used in the study**

104   Bacterial strains and primers used in this study are listed in **Table 1**. *S. aureus* and
105 *Escherichia coli* were routinely grown in LB or TSB medium, respectively, at 37°C with shaking.
106 The media were supplemented with antibiotics, as required.

107

108 **Table 1: Bacterial strains, plasmids, and primers used in the study**

Bacteria	Relevant characteristics	Source
S. aureus Newman		(17)
S. aureus RN4220		(18)
E. coli HST08		Takara
Plasmids and Phage		
pND50-P*fbaA*	pND50 consisting constitutive *fbaA* promoter	(19, 20)
pSF151		(21)
pKOR3a		(22)
Phage 80α		(23)
Primers	**Sequence (5'-3')**	
Disruption of *rsaC*		
rsaC_U_F	GCCCTTCAGTTTTTCATCA	
rsaC_U_R	GTTCGCTAGATAGGGGTCCCCCACCAAAGCGAAGTTTA	
rsaC_D_F	ATCACCTCAAATGGTTCGCTTTGTTATGTTGATGTGTGGC	
rsaC_D_R	TAAACAAGATCCACACGCA	
KmF	AGCGAACCATTTGAGGTGAT	

4

KmR	GGGACCCCTATCTAGCGAAC
rsaC complementation	
rsaC_bam_F	CGC<u>GGATCC</u>GCACGATATGGTGGTATTAG
rsaC_sal_R	ACGC<u>GTCGAC</u>TGAAAAACTGAAGGGCTT
RT-PCR	
16s_rRNA_F	CAACGCGAAGAACCTTACCAA
16s_rRNA_R	GCGGGACTTAACCCAACATCT
rsaC_RT_F	AGGGAATGGCGTTGTATAAATTG
rsaC_RT_R	TCGTTCCCTTCATCTCTTTTAACC

109

Real-time RT-PCR

111   According to the manufacturer's recommendations, one microgram of RNA was used to
112 prepare cDNA using a High-Capacity RNA-to-cDNA^{TM} Kit (Applied Biosystems; Foster City, CA,
113 USA). From this, 15 ng of the cDNA was used as a template for RT-PCR using Fast SYBR Green
114 Master Mix (Thermo Fisher Scientific) on a 7500 Fast (Applied Biosystems) machine with 40
115 cycles of denaturing at 95 ˚C followed by annealing/extension at 60 ˚C.

116

Construction of Δ*rsaC* strain and complementation

118   *rsaC* was disrupted using a double cross-over recombination method as previously described
119 (24). Briefly, the genome regions up-and down-stream of *rsaC* were amplified by PCR using the
120 listed primers. Then, overlap extension-PCR was performed using these two DNA fragments
121 together with the *aph* gene amplified from the pSF151 vector using primers KmF and KmR. The
122 PCR product was cloned into the pKOR3a vector (24) and introduced into the RN4220 strain (18)
123 by electroporation. Integration of the mutant cassette in the genome was confirmed by PCR and
124 further transformed into *S. aureus* Newman (17) by phage transduction using phage 80α as
125 previously described (23, 25).

126

127   To prepare the overexpression strain, the *rsaC* coding region was amplified by the primer
128 pair rsaC_bam_F and rsaC_sal_R (**Table 1**) and ligated to BamHI-SalI digested pND50-P*fbaA* (19,
129 20). The resulting plasmid, pND50-P*fbaA-rsaC*, was then transformed into *S. aureus* RN4220 by
130 electroporation and then to *S. aureus* Newman wild and Δ*rsaC* strains by phage transduction.

131

Proteolytic and hemolytic assays

133   Bacteria were grown overnight in TSB medium, supplemented with antibiotics, as required,
134 at 37°C with shaking. From this, 2 μl aliquots were spotted on TSB containing 3.3% skim milk or
135 sheep blood agar plates (E-MR93; Eiken Chemical, Tokyo, Japan) to determine proteolysis and
136 hemolysis, respectively. The plates were incubated at 37°C overnight. Sealed container with Anaero
137 Pack (Mitsubishi Gas Chemical, Tokyo, Japan) were used to determine phenotypes under anaerobic

138   conditions. The proteolytic and hemolytic activities were determined by the appearance of a clear

139   zone surrounding the bacterial growth.

140

141   **Mouse survival assay**

142   *S. aureus* Newman wild-type and Δ*rsaC* strains were grown overnight on TSB medium

143   supplemented with antibiotics, as required, on a rotary shaker maintained at 37 ˚C to obtain full

144   growth. The full growth was diluted 100-fold with TSB and cultured overnight on the same shaker,

145   and then the cells were centrifuged and resuspended in phosphate-buffered saline (PBS, pH 7.2) to

146   have an optical density (OD_{600}) of 0.7. An aliquot (200 µl) of the prepared cell suspension was then

147   injected intravenously into C57BL/6J mouse, and mouse survival was observed. Survival analysis

148   was performed using GraphPad Prism ver 8.0 (GraphPad Software), and statistical analysis was

149   performed using the Log-rank (Mantel-Cox) test.

150

151   *S. aureus* **infection, organ isolation and RNA isolation**

152   *Staphylococci* were grown overnight on TSB medium at 37˚C with shaking. The full growth

153   was diluted 100-fold with 5 ml TSB and regrown for 16h under the same conditions. The cells were

154   centrifuged and suspended in PBS (pH 7.2). The cells (OD_{600} = 0.7) were injected into C57BL/6J

155   mice via the tail vein. On day 1, mice were killed to harvest organs. Organs were immediately

156   placed either in ice to calculate viable cell numbers in each organ or liquid nitrogen and maintained

157   at -80 ˚C for RNA extraction. Each experiment was conducted with three animals, and data are

158   represented as an average. Mouse organs were homogenized, and total RNA was extracted, as

159   explained previously (6). RNA extraction from *in vitro* culture was performed as explained (19).

160   For anaerobic RNA-Seq, staphylococci were first grown aerobically to reach OD_{600} of 1.0 and then

161   transferred to anaerobic growth for 30 minutes.

162

163   **Library preparation and RNA-sequencing**

164   Total RNA was subjected to rRNA depletion using a MICROBExpress[TM] Kit (Thermo

165   Fisher Scientific, Waltham, MA) and used for library preparation for RNA-Seq using an Ion Total

166   RNA-Seq Kit v2 following the manufacturer's instructions. After confirming the size distribution

167   and yield of the amplified library using a bioanalyzer, the libraries were enriched in an Ion PI Chip

168   v2 using the Ion Chef (Thermo Fisher Scientific) and sequenced using Ion Proton System (Thermo

169   Fisher Scientific). These data have been deposited in the NCBI Sequence Read Archive under

170   accession number ######.

171

172   **Differential gene expression analysis**

6

173   All data were analyzed using CLC Genomics Workbench software, version 21.0.4 (CLC

174 Bio, Aarhus, Denmark). Reads were aligned to the Newman genome annotated with ncRNA genes

175 allowing a minimum length fraction of 0.95 and a minimum similarity fraction of 0.95. Differential

176 gene expression analysis was performed using the default setting. Genes with a false discovery rate

177 (FDR) $p<0.05$ were classified as having significantly different expressions.

178

179 **Results**

180 **Comprehensive analysis of sRNAs expression in the host environment**

181   To quantitatively analyze the expression of *S. aureus* sRNAs within the host, we first

182 annotated the sRNAs present in the Newman strain based on the report of Sassai *et al.* (11). Next,

183 we performed an RNA-Seq analysis based on the reads obtained from our two-step cell crush

184 method (6). A comparative expression analysis of RNA isolated from host liver at 6- hr, 1- day and

185 2- day post-infection to the RNA isolated from *in-vitro* culture was performed. We found that

186 among 559 sRNAs present, 34 sRNAs were differentially expressed at all the three-time points

187 compared to *in vitro* (**Figure 1**). Upregulation or downregulation of these sRNAs at all three time

188 points suggested these sRNAs' possible role to respond to host circumstances.

7
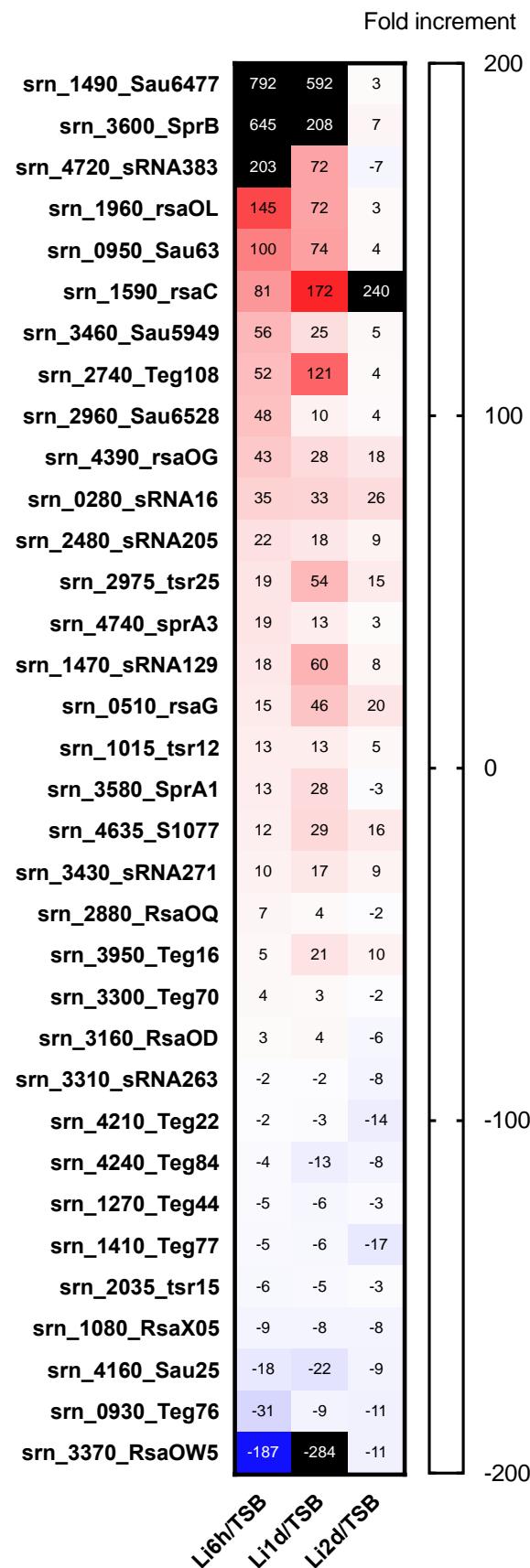
Figure 1. Expression of staphylococcal sRNAs in the host environment. Differential expression of Newman sRNAs in mouse liver compared to TSB medium culture condition. sRNAs with common differential expression and FDR p < 0.05 on all the three-time points are shown.

193

Identification of RsaC as a virulence factor

Given that many sRNAs were differentially expressed under the host circumstances, we were interested in whether these sRNAs can modulate *S. aureus* pathogenesis. Among sRNAs, we focused on *rsaC*, as it falls among one of the studied staphylococcal sRNAs. Previously, *rsaC* was shown to have an increased expression in the infected host (15) and modulate oxidative stress during manganese starvation (16). However, its role in the regulation of pathogenesis has remained elusive. First, we confirmed the expression of *rsaC* in mouse organs using a real-time reverse transcription-polymerase chain reaction (RT-PCR). A higher expression of *rsaC* was observed in both the kidney and liver, as compared to TSB medium culture condition (**Figure 2A**). The gene organization of *rsaC* in the Newman genome (**Figure 2B**) showed that *rsaC* did not overlap with other genes, allowing us to construct a single gene disruption mutant. We constructed the *rsaC* disrupted mutant and examined its role in pathogenicity using a mouse infection model. We found that Δ*rsaC* had reduced ability to colonize in mouse heart 24h post-infection whereas the ability to colonize in kidney, liver, lungs and spleen were indistinguishable from that of the wild-type (**Figure 2C**). To further confirm the role of *rsaC* in virulence, we checked the survival of wild-type or Δ*rsaC*- infected mice. The results indicated that the Δ*rsaC* strain had reduced virulence (**Figure 2D**), evident by prolonged survival of the Δ*rsaC* infected mice. To eliminate the possibilities of polar effects associated with this disruption on pathogenicity, we complemented the wild-type and the Δ*rsaC* strains by reintroducing *rsaC* under the control of a constitutive promoter- P*fbaA*. Restored pathogenicity of the complemented strain unequivocally explained the involvement of *rsaC* in pathogenicity and established it as a virulence factor of *S. aureus*.
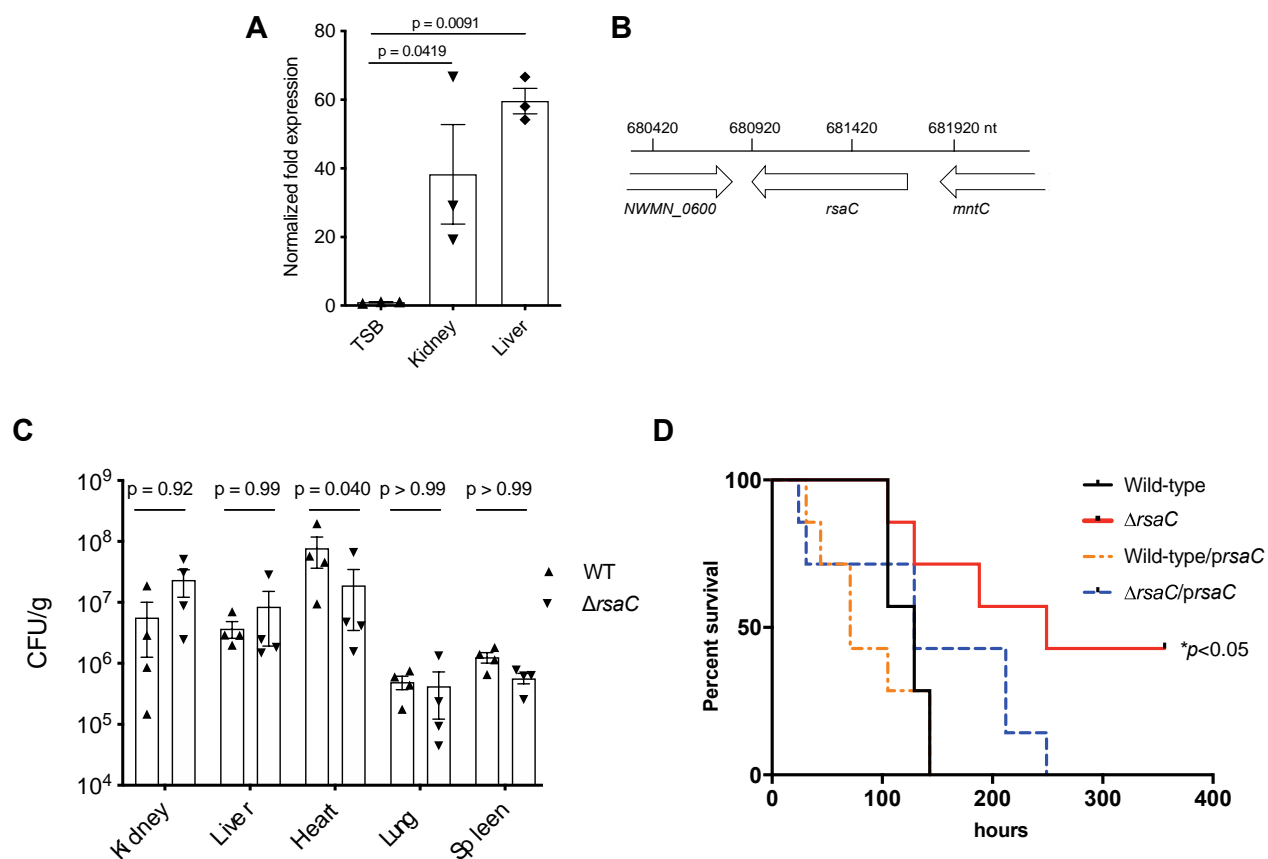
215

Figure 2. *In vivo* expression and involvement of RsaC in the pathogenesis of *S. aureus.* (A) Upregulation of *rsaC* in host organs compared with that in TSB medium was confirmed by RT-PCR. The data were standardized by the abundance of 16s rRNA in each sample, and statistical analysis was performed using ANOVA. (B) Position of the *rsaC* in *S. aureus* Newman chromosome. (C) The number of *S. aureus* cells in each organ after infection with (7.6×10^7 CFU and 7.5×10^7 CFU) *S. aureus* Newman and Δ*rsaC* strains, respectively. Statistical analysis was performed using 2way ANOVA with Sidak's multiple comparisons in GraphPad Prism 8.4.3. (D) Survival of mice after the infection with a deletion mutant of the *rsaC* gene. Wild-type, Δ*rsaC*, wild-type/p*rsaC*, or Δ*rsaC*/p*rsaC* were injected intravenously at a dose of 5.0×10^7, 5.9×10^7, 4.8×10^7 and 5.0×10^7 CFU, respectively. Asterisk indicates a significant difference compared with the survival curve following wild-type injection ($p<0.05$) by the Log-rank (Mantel-Cox) test. The experiment was performed two times, and essentially the same results were obtained.

Next, we performed the phenotypic evaluation of the Δ*rsaC* mutant *in vitro*. We found that the growth of Δ*rsaC* strain was indistinguishable from that of the wild-type during both aerobic (**Figure 3A**) and anaerobic (**Figure 3B**) growth. In addition, Δ*rsaC* had unaltered proteolytic and hemolytic abilities compared to that of the wild-type during both aerobic and anaerobic culture conditions (**Figure 3C, D**). These results suggested no difference between the wild-type and mutant

235   in terms of virulence-related *in vitro* phenotypes and necessitated an *in vivo* infection system to

236   investigate the role of *rsaC* in pathogenesis.

237

238
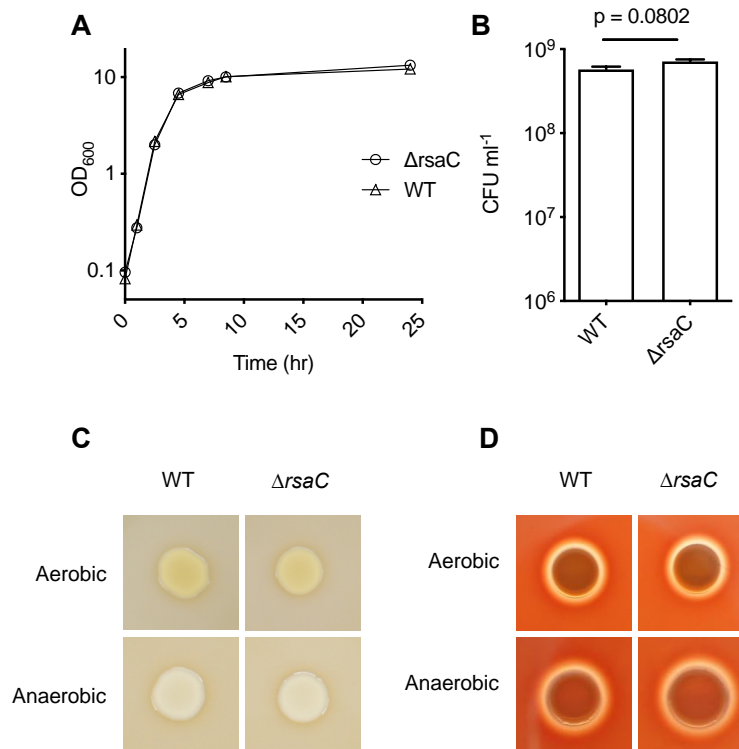
Figure 3. *In vitro* phenotypic analysis of *rsaC* disruption.

240   (A) Growth curve of Δ*rsaC* and wild-type strains during aerobic culture. (B) Colony Forming

241   Units (CFUs) of Δ*rsaC* and wild-type strains after growing anaerobically. Statistical analysis was

242   performed using an unpaired t-test. (C) Proteolytic- and (D) hemolytic- ability of Δ*rsaC* and wild-

243   type strains during aerobic and anaerobic conditions.

244

Role of *rsaC* in *S. aureus* transcriptome

246   Given that *in vitro* phenotypic analysis could not elucidate the possible link between the

247   *rsaC* disruption and pathogenicity, we aimed to examine the transcriptome at the global level. We

248   compared the gene expression pattern by performing an RNA-Seq analysis of the Δ*rsaC* and the

249   wild-type strains under multiple growth conditions- aerobic, anaerobic, and *in vivo* (**Figure 4A**).

250   Since we found higher colonization of *S. aureus* in the heart compared to other organs, and the

251   Δ*rsaC* strain tended to colonize less in the heart compared to the wild-type (**Figure 2D**), we

252   selected heart for *in vivo* RNA-Seq. The gene expression patterns of the Δ*rsaC* strain was compared

253   to that of the wild-type strain in different growth conditions revealing the differential expression of

254   diverse genes in the three tested conditions. Whereas 29, 254, and 47 genes were differentially

255   expressed on RNA obtained from aerobic-growth, anaerobic-growth, and mouse heart, respectively,

256   no commonly affected genes were observed (**Figure 4B**). This indicated a difference in the gene

11

257 expression pattern depending on growth conditions. Fermentation-related genes, most of which are

258 also associated with the oxidoreductase activity, were downregulated in the Δ*rsaC* mutant when

259 grown under aerobic conditions (**Figure 4C, Table 2**). Based on this, we speculated that *rsaC*

260 directs *S. aureus* towards fermentative respiration by acting as a regulator of fermentation. Under

261 anaerobic conditions, we found the downregulation of many transporters, virulence-related genes in

262 Δ*rsaC* mutant (**Figure 4D, Table 2**). The *in vivo* RNA-Seq analysis, performed in mouse heart at

263 24 -hr post-infection, showed that compared to wild-type strains, genes related to metal ion (copper

264 and potassium) acquisition and virulence (related to tissue invasion, evasion of host defense, and

265 inhibition of neutrophil activation) were significantly downregulated in the Δ*rsaC* strain (**Figure 4E,**

266 **Table 2**), which suggested the possible role of host stress towards pathogen response. Taken

267 together, these results indicate the diverse functions of *rsaC* during aerobic, anaerobic, and *in vivo*

268 growth.

269

270 We further categorized the differentially expressed genes depending on their up-and down-

271 regulated status and performed a PANTHER overrepresentation test. We found that genes related to

272 oxidoreductase activity were overrepresented among the genes downregulated in aerobic conditions

273 (**Table 3**). Conversely, among the genes upregulated during the anaerobic condition, the genes

274 related to protein folding and translation were overrepresented, and the genes involved in

275 transmembrane transport were underrepresented (**Table 3**). A previous study also found that these
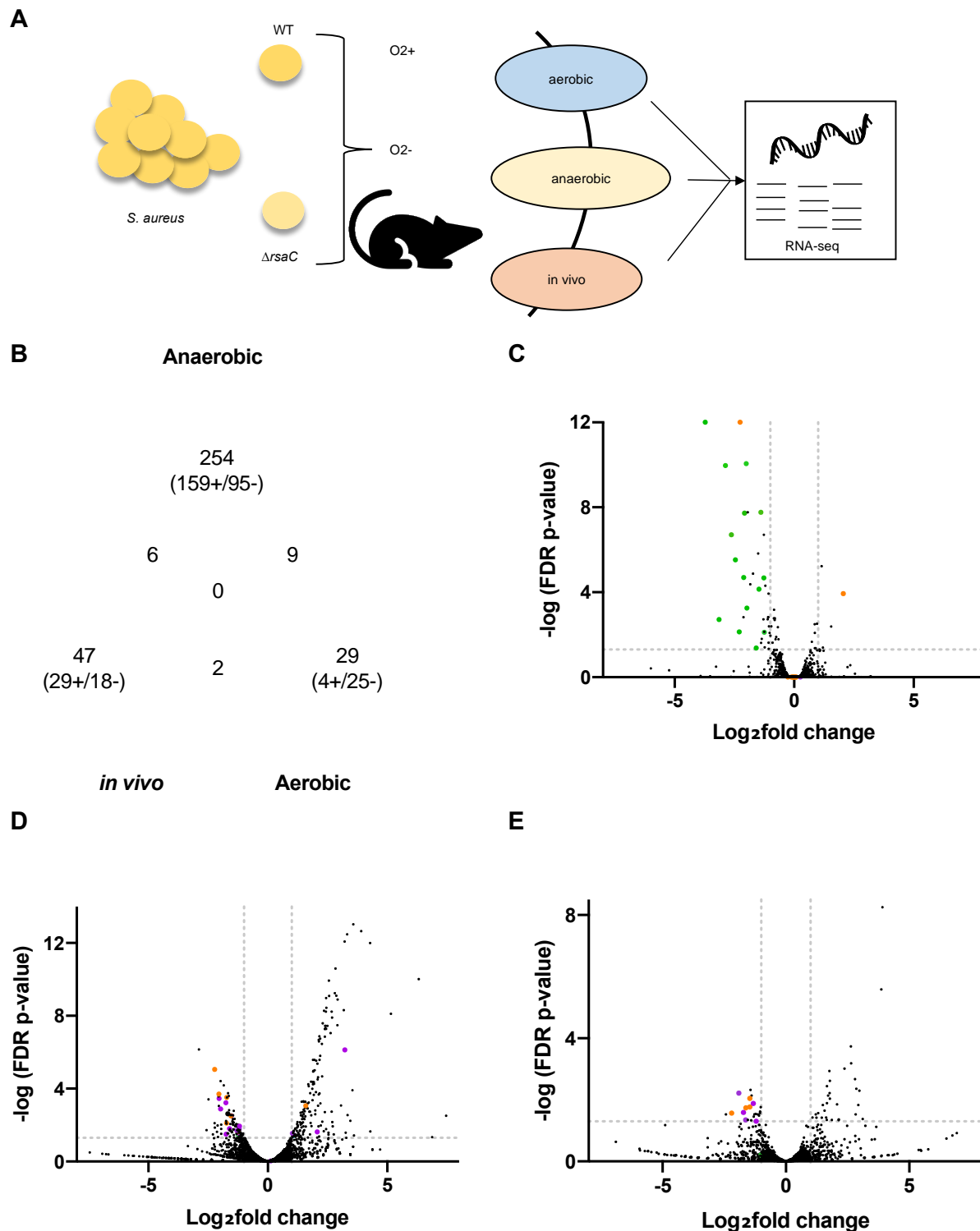
276 genes are upregulated in anaerobic conditions (26).

277

Figure 4. Global transcriptomic analysis of rsaC disruption in *S. aureus*. (**A**) Experimental model to perform transcriptomic analysis. (**B**) Venn diagram showing the genes with common differential expression between *in vitro* (aerobic and anaerobic) and *in vivo* (heart). A volcano plot showing the genes differentially expressed in the Δ*rsaC* strain, compared to wild-type during (**C**) aerobic, (**D**) anaerobic, and (**E**) *in vivo* (heart) growth. Genes involved in fermentation, virulence, and metal-ion acquisition are colored green, orange, and purple, respectively. Data points outside the dotted lines along the y-axis represent fold changes of ≥ 2.0 and that along the x-axis represent

13

286 FDR $p \leq 0.05$. The complete list of differentially expressed genes is presented in the supplementary

287 dataset.

288

289 **Table 2: Fermentation, virulence, and metal ion acquisition-related genes differentially**

290 **expressed (FDR p < 0.05 in the $\Delta rsaC$ strain compared to wild-type) during aerobic,**

291 **anaerobic, and *in vivo* growth.**

Gene name	Gene product	$\Delta rsaC$ vs. WT during					
		aerobic		anaerobic		*in vivo*	
		Fold	FDR p	Fold	FDR p	Fold	FDR p
Category: Fermentation							
pflB	formate acetyltransferase	**-13.18**	0.00	1.50	0.44	-1.23	0.90
lctE	L-lactate dehydrogenase	**-8.84**	0.00	2.13	0.04	-1.60	0.76
pflA	pyruvate formate-lyase-activating enzyme	**-7.33**	0.00	2.40	0.03	-1.22	0.90
nirR	cobalamin biosynthesis protein CbiX	**-6.18**	0.00	1.51	0.43	-1.28	0.88
lctP	L-lactate permease	**-5.48**	0.00	-1.85	0.13	-1.12	0.95
adh1	zinc-dependent alcohol dehydrogenase	**-4.32**	0.00	2.31	0.02	-1.68	0.69
ilvA	serine/threonine dehydratase	**-4.22**	0.00	-1.99	0.10	-1.72	0.56
nasD, nirB	nitrite reductase large subunit	**-4.02**	0.00	1.13	0.87	-1.24	0.88
ald	alanine dehydrogenase	**-3.95**	0.00	-1.24	0.72	-1.83	0.47
nasE, nirD	nitrite reductase (NAD(P)H) small subunit	**-3.00**	0.04	-1.51	0.40	-1.38	0.85
adhE	bifunctional acetaldehyde-CoA/alcohol dehydrogenase	**-2.77**	0.00	-1.27	0.70	-1.85	0.62
ddh	lactate dehydrogenase	**-2.63**	0.00	1.37	0.49	1.05	0.98
ndhF	NADH dehydrogenase subunit 5	**-2.40**	0.00	-1.08	0.93	1.19	0.93
NWMN_RS13240	formate/nitrite transporter	-1.03	1.00	**-2.39**	0.03	-1.34	0.76
NWMN_RS01365	formate/nitrite transporter	**-4.92**	0.01	-1.44	0.43	1.14	0.91
narK, narT	MFS transporter	**-2.37**	0.01	1.11	0.90	-2.02	0.63
Category: Virulence							
ccpA	catabolite control protein A	1.05	1.00	**-4.69**	0.00	1.02	0.99
agrB	accessory gene regulator AgrB	-1.06	1.00	**-4.14**	0.00	-1.97	0.53
hlgB	gamma-hemolysin component B	-1.08	1.00	**-3.30**	0.01	-1.73	0.84
lukF	Leukocidin/Hemolysin toxin family protein	-1.02	1.00	**-3.29**	0.00	-1.07	0.98
mgrA	MarR family transcriptional regulator	1.04	1.00	**-3.20**	0.00	-1.27	0.88
lukS	Aerolysin/Leukocidin family protein	1.01	1.00	**-2.91**	0.00	-1.09	0.98
agrC	ATP-binding protein	-1.04	1.00	**-2.40**	0.02	-1.77	0.76
sak	staphylokinase			-1.93	0.73	**-4.59**	0.03
sspB	staphopain A	1.06	1.00	-1.15	0.91	**-3.09**	0.02
eta	permease	-1.20	1.00	-1.32	0.64	**-2.75**	0.02
nsaS		-1.02	1.00	-1.02	0.98	**-2.76**	0.01
spa	peptidoglycan-binding protein LysM	**-4.80**	0.00	**3.00**	0.00	1.64	0.45
Category: Metal-ion acquisition							
opuCD	amino acid ABC transporter permease	1.20	1.00	**-3.38**	0.00	1.26	0.82
NWMN_RS03330	iron ABC transporter permease	-1.06	1.00	**-3.36**	0.03	-1.08	0.94
NWMN_RS09470	calcium-binding protein	-1.81	0.08	**-3.04**	0.02	-1.69	0.51

Gene	Description						
NWMN_RS12570	molybdenum cofactor biosynthesis protein	1.13	1.00	**-2.29**	0.02	1.08	0.96
copZ	copper chaperone CopZ	1.06	1.00	1.76	0.45	**-3.30**	0.03
narJ	nitrate reductase molybdenum cofactor assembly chaperone	1.11	1.00	**-4.11**	0.00	-1.64	0.84
NWMN_RS03330	iron ABC transporter permease	-1.06	1.00	**-3.36**	0.03	-1.08	0.94
NWMN_RS09470	calcium-binding protein	-1.81	0.08	**-3.04**	0.02	-1.69	0.51
mnhC, mnhC1	Na(+)/H(+) antiporter subunit C	-1.03	1.00	**-3.93**	0.00	1.10	0.93
NWMN_RS08175	MBL fold metallo-hydrolase	1.09	1.00	**2.04**	0.03	-1.19	0.88
putP	sodium:proline symporter	1.02	1.00	**-2.45**	0.02	1.10	0.93
cobI	magnesium transporter CorA	1.14	1.00	**-2.39**	0.03	-1.12	0.91
sirA	iron ABC transporter substrate-binding protein	-1.17	1.00	**4.18**	0.02	-1.06	0.97
sitC, mntC	metal ABC transporter substrate-binding protein	1.68	0.02	**9.32**	0.00	1.76	0.63
NWMN_RS03420	sodium:proton antiporter	1.10	1.00	**-2.28**	0.01	**-2.49**	0.01
czrB	cation transporter	1.07	1.00	**-2.88**	0.00	**-2.30**	0.05
kdpB	potassium-transporting ATPase subunit B	1.26	0.86	1.09	0.95	**-3.09**	0.04
czrAf	zinc/cobalt-responsive transcriptional repressor	1.164	0.999	-1.1	0.901	**-3.7**	0.006

292

Table 3: Significantly overrepresented or underrepresented groups among the genes differentially expressed in the Δ*rsaC* strain.

Downregulated in aerobic	Fold Enrichment	FDR p
GO molecular function		
oxidoreductase activity	4.83	3.63E-02
Upregulated in anaerobic	**Fold Enrichment**	**FDR p**
GO biological process		
'de novo' protein folding	21.89	2.17E-02
protein folding	15.92	8.31E-05
chaperone-mediated protein folding	21.89	2.06E-02
translation	6.65	1.99E-12
peptide biosynthetic process	6.11	7.24E-12
peptide metabolic process	5.61	3.62E-11
organonitrogen compound metabolic process	1.85	1.51E-03
cellular amide metabolic process	4.19	5.64E-09
cellular nitrogen compound metabolic process	1.71	3.41E-02
amide biosynthetic process	5.27	4.43E-11
cellular nitrogen compound biosynthetic process	2.67	1.27E-05
organonitrogen compound biosynthetic process	2.24	5.30E-04
organic substance biosynthetic process	1.71	4.55E-02
gene expression	3.59	1.77E-07
macromolecule metabolic process	1.93	1.18E-03
cellular macromolecule biosynthetic process	3.25	7.92E-07
cellular macromolecule metabolic process	2.18	2.78E-04
macromolecule biosynthetic process	3.22	8.76E-07
cellular protein metabolic process	4.28	1.78E-10
protein metabolic process	3.66	2.32E-10
primary metabolic process	1.54	3.27E-02
transmembrane transport	0.08	7.89E-03
GO molecular function		
unfolded protein binding	14.59	6.33E-03
structural constituent of ribosome	11.14	2.09E-16
structural molecule activity	11.14	1.05E-16
rRNA binding	8.65	1.02E-07
RNAbinding	3.91	4.99E-05
transmembrane transporter activity	0.09	3.83E-02
transporter activity	0.09	3.29E-02
GO cellular component		
cytosolic large ribosomal subunit	10.1	3.92E-07
cytosolic ribosome	9.85	2.30E-10
cytosol	2.25	3.31E-04
cytoplasm	1.84	1.15E-04
intracellular anatomical structure	2.13	1.79E-08
ribosome	10.94	1.70E-18

intracellular non-membrane-bounded organelle	8.75	3.74E-17
intracellular organelle	7.45	2.68E-16
organelle	7.45	2.14E-16
non-membrane-bounded organelle	8.75	2.50E-17
large ribosomal subunit	9.73	5.07E-07
ribosomal subunit	9.12	6.07E-11
ribonucleoprotein complex	8.58	1.28E-10
protein-containing complex	2.74	2.04E-04
cytosolic small ribosomal subunit	9.38	1.17E-03
small ribosomal subunit	8.34	2.11E-04
integral component of membrane	0.22	3.18E-07
intrinsic component of membrane	0.22	2.94E-07
membrane	0.2	7.28E-09
plasma membrane	0.21	4.02E-04
cell periphery	0.25	9.19E-04

295

296 **Discussion**

297

298 In this manuscript, we identified a Staphylococcal sRNA *rsaC* as a virulence factor, required for

299 full virulence of *S. aureus*. Despite some studies involving *rsaC* (15, 16), its participation in

300 pathogenesis was obscure. Our results suggested that RsaC regulates *S. aureus* transcriptome

301 differently, depending on oxygen availability and host stress. For instance, during aerobic

302 conditions where cells tend to use O_2 as a terminal electron acceptor (27, 28), we found that RsaC

303 was directing the cells towards anaerobic respiration. Besides, anaerobic conditions, such as those

304 encountered *in vivo* and exaggerated by pathogen colonization and heart failure (6) might lead to

305 the adaptation to adverse environment by regulating nutrition acquisition and virulence factor

306 production, at least partly by the sRNA *rsaC*.

307

308 We also found that many genes involved in metal acquisition were downregulated during

309 anaerobic and *in vivo* conditions. Lalaouna et al elucidated the role of *rsaC* in regulating oxidative

310 stress during manganese starvation and identified an Mn-dependent superoxide dismutase *sodA*

311 mRNA as the target of *rsaC* (16). They also found that RsaC interacts of *sodA* mRNA and affects

312 the posttranslational events (16). In our RNA-Seq analysis, we did not find the differential

313 expression of *sodA* in any of the three different growth conditions tested, indicating that *rsaC* does

314 not affect *sodA* at transcriptional level. Thus, our approach of comparing less-virulent strain with its

315 counter virulent strain under different conditions led to the findings that *rsaC* has diverse roles

316 dependent upon the environment encountered by *S. aureus*, yet there existed some commonalities.

317 The gene expression in aerobic condition implied that *rsaC* was involved in shifting bacterial cells

318 from aerobic to anaerobic respiration state; that in anaerobic condition revealed that *rsaC* was

319 involved in metal acquisition and toxin production; and that during *in vivo* condition uncovered that

320 *rsaC* was involved in virulence through host invasion and inhibiting the activation of neutrophils.

321 Therefore, based on previous study (16) and this study, RsaC functions as a transcriptional and

16

322 translational regulator of a wide variety of genes (**Figure 5**) which ultimately play a role in
323 virulence, a detailed mechanism of which is yet to be identified.
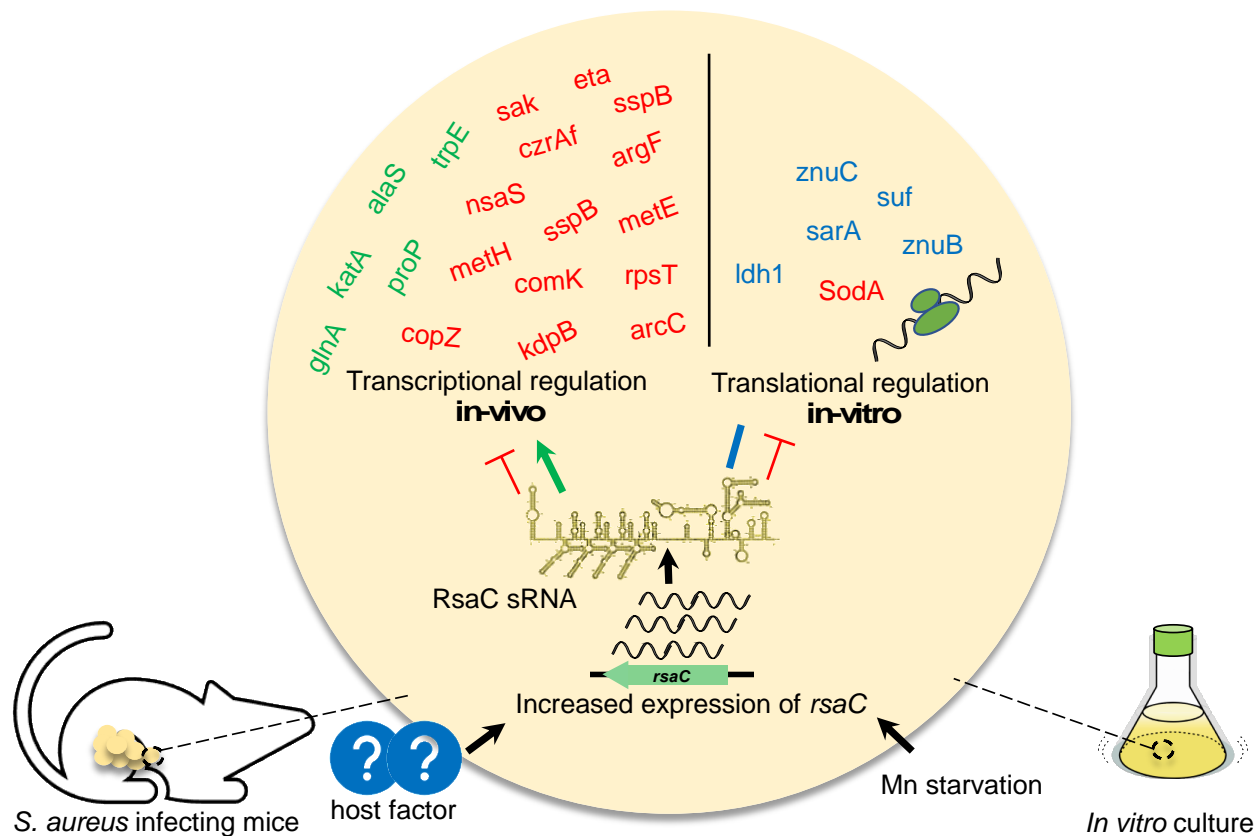
324
325 **Figure 5**. Role of RsaC in gene regulation *in vivo* and *in vitro*. Unknown host factors (*in vivo*) or
326 Mn starvation (*in vitro*) trigger the expression of *rsaC*, which regulates the expression of several
327 genes (this study) or binds to several mRNAs and regulate their translation (16). Red, green, and
328 blue color indicate negative regulation, positive regulation, and binding with unknown effect,
329 respectively.

330

331   Further, we observed the upregulation of genes involved in translation, protein folding, and
332 oxidative stress during anaerobic condition. Since clear role of these genes in virulence remains
333 unknown, we speculate that the regulation of translation and protein folding could be a secondary
334 effect of *rsaC* disruption. For instance, in manganese depleted environment, *rsaC* modulated SodM
335 that can use iron as the cofactor for ROS detoxification (16). A detailed understanding of *rsaC*
336 upregulation inside hosts and how RsaC controls gene expression at transcriptional, translational,
337 and posttranslational levels requires further investigation. We searched for partially homologous
338 sequences to the *rsaC* gene in whole genome sequence of the Newman strain that could be targets
339 of transcriptional regulation by RsaC, however; were unable to find any regions. Nonetheless, this
340 key finding of the involvement of RsaC in the virulence of *S. aureus* led to the identification of

341 novel virulence sRNA and opened up avenues for the development of novel antimicrobial agents to

342 treat severe systemic infection by targeting the RsaC signaling pathway.

343

344 **Acknowledgements**

349

350

351 **Author contributions**

352 S.P. and H.H. conceived the idea. S.P., H.H. and A.P. performed *in vivo* RNA-Seq analysis. S.P.

353 and A.P. wrote the manuscript. S.O. prepared the gene disruptant mutants. H.H., S.P., A.P., and S.O.

354 performed the mouse systemic infection assays. S.P. performed real time RT-PCR and *in vitro*

355 phenotypic analysis. K.S. critically revised the article for important intellectual content and

356 provided final approval of the article.

357

358 **Competing interests**

359 K.S. is a consultant for Genome Pharmaceutical Institute Co., Ltd.

360

361 **References**

362 1.   Colgan AM, Cameron AD, Kroger C. 2017. If it transcribes, we can sequence it: mining the
363   complexities of host-pathogen-environment interactions using RNA-seq. Curr Opin
364   Microbiol 36:37-46.
365 2.   Creecy JP, Conway T. 2015. Quantitative bacterial transcriptomics with RNA-seq. Curr
366   Opin Microbiol 23:133-40.
367 3.   Ishii K, Adachi T, Yasukawa J, Suzuki Y, Hamamoto H, Sekimizu K. 2014. Induction of
368   virulence gene expression in *Staphylococcus aureus* by pulmonary surfactant. Infect Immun
369   82:1500-1510.
370 4.   Westermann AJ, Förstner KU, Amman F, Barquist L, Chao Y, Schulte LN, Müller L,
371   Reinhardt R, Stadler PF, Vogel J. 2016. Dual RNA-seq unveils noncoding RNA functions in
372   host–pathogen interactions. Nature 529:496-501.
373 5.   Hirose Y, Yamaguchi M, Okuzaki D, Motooka D, Hamamoto H, Hanada T, Sumitomo T,
374   Nakata M, Kawabata S. 2019. Streptococcus pyogenes Transcriptome Changes in the
375   Inflammatory Environment of Necrotizing Fasciitis. Appl Environ Microbiol 85.
376 6.   Hamamoto H, Panthee S, Paudel A, Suguru O, Suzuki Y, Sekimizu K. 2021. Transcriptome
377   change in *Staphylococcus aureus* in infecting mice. Nature Portfolio doi:10.21203/rs.3.rs-
378   636230/v1.

379   7.   D'Mello A, Riegler AN, Martinez E, Beno SM, Ricketts TD, Foxman EF, Orihuela CJ,
380   Tettelin H. 2020. An in vivo atlas of host-pathogen transcriptomes during Streptococcus
381   pneumoniae colonization and disease. Proc Natl Acad Sci U S A 117:33507-33518.
382   8.   Caldelari I, Chao Y, Romby P, Vogel J. 2013. RNA-Mediated Regulation in Pathogenic
383   Bacteria. Cold Spring Harbor Perspectives in Medicine 3.
384   9.   Guillet J, Hallier M, Felden B. 2013. Emerging functions for the *Staphylococcus aureus*
385   RNome. PLOS Pathog 9:e1003767.
386   10.   Kaito C, Omae Y, Matsumoto Y, Nagata M, Yamaguchi H, Aoto T, Ito T, Hiramatsu K,
387   Sekimizu K. 2008. A novel gene, *fudoh*, in the SCC*mec* region suppresses the colony
388   spreading ability and virulence of *Staphylococcus aureus*. PLoS One 3:e3921.
389   11.   Sassi M, Augagneur Y, Mauro T, Ivain L, Chabelskaya S, Hallier M, Sallou O, Felden B.
390   2015. SRD: a *Staphylococcus* regulatory RNA database. RNA 21:1005-1017.
391   12.   Boisset S, Geissmann T, Huntzinger E, Fechter P, Bendridi N, Possedko M, Chevalier C,
392   Helfer AC, Benito Y, Jacquier A, Gaspin C, Vandenesch F, Romby P. 2007. Staphylococcus
393   aureus RNAIII coordinately represses the synthesis of virulence factors and the transcription
394   regulator Rot by an antisense mechanism. Genes Dev 21:1353-66.
395   13.   Huntzinger E, Boisset S, Saveanu C, Benito Y, Geissmann T, Namane A, Lina G, Etienne J,
396   Ehresmann B, Ehresmann C, Jacquier A, Vandenesch F, Romby P. 2005. Staphylococcus
397   aureus RNAIII and the endoribonuclease III coordinately regulate spa gene expression.
398   EMBO J 24:824-35.
399   14.   Gupta RK, Luong TT, Lee CY. 2015. RNAIII of the Staphylococcus aureus agr system
400   activates global regulator MgrA by stabilizing mRNA. Proc Natl Acad Sci U S A
401   112:14036-41.
402   15.   Szafranska AK, Oxley APA, Chaves-Moreno D, Horst SA, Roßlenbroich S, Peters G,
403   Goldmann O, Rohde M, Sinha B, Pieper DH, Löffler B, Jauregui R, Wos-Oxley ML,
404   Medina E. 2014. High-resolution transcriptomic analysis of the adaptive response of
405   *Staphylococcus aureus* during acute and chronic phases of osteomyelitis. mBio 5.
406   16.   Lalaouna D, Baude J, Wu Z, Tomasini A, Chicher J, Marzi S, Vandenesch F, Romby P,
407   Caldelari I, Moreau K. 2019. RsaC sRNA modulates the oxidative stress response of
408   Staphylococcus aureus during manganese starvation. Nucleic Acids Res 47:9871-9887.
409   17.   Duthie ES, Lorenz LL. 1952. Staphylococcal coagulase; mode of action and antigenicity. J
410   Gen Microbiol 6:95-107.
411   18.   Peng HL, Novick RP, Kreiswirth B, Kornblum J, Schlievert P. 1988. Cloning,
412   characterization, and sequencing of an accessory gene regulator (*agr*) in *Staphylococcus
413   aureus*. J Bacteriol 170:4365-72.
414   19.   Paudel A, Panthee S, Hamamoto H, Grunert T, Sekimizu K. 2021. YjbH regulates virulence
415   genes expression and oxidative stress resistance in *Staphylococcus aureus*. Virulence
416   12:470-480.
417   20.   Paudel A, Hamamoto H, Panthee S, Matsumoto Y, Sekimizu K. 2020. Large-Scale
418   Screening and Identification of Novel Pathogenic *Staphylococcus aureus* Genes Using a
419   Silkworm Infection Model. J Infect Dis 221:1795-1804.
420   21.   Tao L, LeBlanc DJ, Ferretti JJ. 1992. Novel streptococcal-integration shuttle vectors for
421   gene cloning and inactivation. Gene 120:105-10.
422   22.   Bae T, Schneewind O. 2006. Allelic replacement in Staphylococcus aureus with inducible
423   counter-selection. Plasmid 55:58-63.
424   23.   Novick RP. 1991. Genetic systems in *staphylococci*. Methods Enzymol 204:587-636.
425   24.   Kaito C, Hirano T, Omae Y, Sekimizu K. 2011. Digestion of extracellular DNA is required
426   for giant colony formation of *Staphylococcus aureus*. Microbial Pathogenesis 51:142-148.
427   25.   Paudel A, Hamamoto H, Panthee S, Kaneko K, Matsunaga S, Kanai M, Suzuki Y, Sekimizu
428   K. 2017. A novel spiro-heterocyclic compound identified by the silkworm infection model
429   inhibits transcription in *Staphylococcus aureus*. Front Microbiol 8:712.

430   26.   Fuchs S, Pané-Farré J, Kohler C, Hecker M, Engelmann S. 2007. Anaerobic Gene
431   Expression in Staphylococcus aureus. Journal of Bacteriology 189:4275-4289.
432   27.   Babcock GT. 1999. How oxygen is activated and reduced in respiration. Proc Natl Acad Sci
433   U S A 96:12971-3.
434   28.   Borisov VB, Verkhovsky MI. 2015. Oxygen as Acceptor. EcoSal Plus 6.
435